Available online at www.sciencedirect.com
ScienceDirect
Polymer Degradation and Stability 92 (2007) 1883–1890
Polymer Degradation and Stability
www.elsevier.com/locate/polydegstab

Characterization of weathered wood–plastic composite surfaces using FTIR spectroscopy, contact angle, and XPS☆

Nicole M. Stark [a,*], Laurent M. Matuana [b]

[a] U.S. Department of Agriculture, Forest Service, Forest Products Laboratory, One Gifford Pinchot Drive, Madison, WI 53726–2398, USA
[b] Department of Forestry, Michigan State University, East Lansing, MI 48824–1222, USA

Received 14 March 2007; received in revised form 21 June 2007; accepted 27 June 2007
Available online 21 July 2007

Abstract

Much of the current growth of wood–plastic composites (WPCs) is due to increased penetration into the decking market; therefore it has become imperative to understand the durability of WPCs in outdoor applications. In this study, wood flour filled high-density polyethylene (HDPE) composites were manufactured through either injection molding or extrusion. A set of extruded composites were also planed to remove the extruded surface. Composites were weathered in a xenon-arc weathering apparatus. Scanning electron microscopy (SEM) was used to characterize the morphology of the composite surface. Attenuated total reflectance Fourier transform infrared (ATR-FTIR) spectroscopy was useful in showing the loss of wood particles from the surface after weathering. Contact angle was higher for the extruded and planed composites compared with the injection molded composites, and was shown using X-ray photoelectron spectroscopy (XPS) to be due to lubricant used as a processing aid.
Published by Elsevier Ltd.

Keywords: Wood–plastic composites; Weathering; Wood flour; HDPE; Mechanical properties; Surface characteristics

1. Introduction

Wood–plastic composites (WPCs) have found their way into consumer, automotive, and construction applications, and are experiencing tremendous growth in exterior residential construction applications. The introduction of WPCs in the decking market is mainly responsible for this growth. There are currently over 30 decking manufacturers on the market, and WPCs are predicted to have 25% of the market by 2009 [1]. WPC lumber is promoted as a lower-maintenance alternative compared with solid wood. WPCs are often seen as green composites, the wood is a renewable component sourced from a waste stream and the entire composite can be recyclable [2]. A direct result of success in the decking market is that products are now being developed and introduced for new exterior applications such as railings, fencing, roofing, and siding.

WPCs are typically comprised of wood or other natural lignocellulosic fibers in a thermoplastic matrix. In North America, polyethylene is the most common thermoplastic used in manufacturing WPCs. Polypropylene, polyvinyl chloride, and polystyrene are also being used. Most WPCs use wood flour as the wood component. Pine, maple, and oak with mesh sizes between 20 and 100 mesh are commonly available for WPCs. Wood flour is typically incorporated into WPCs at 50–60% by weight.

The manufacture of WPCs commonly includes two steps: compounding and forming. During compounding, wood and

☆ The Forest Products Laboratory is maintained in cooperation with the University of Wisconsin. This article was written and prepared by U.S. Government employees on official time and is therefore in the public domain and not subject to copyright. Use of trade or firm names in this publication is for reader information and does not imply endorsement by the U.S. Department of Agriculture of any product or service.

* Corresponding author.
E-mail address: nstark@fs.fed.us (N.M. Stark).

0141-3910/$ - see front matter Published by Elsevier Ltd.
doi:10.1016/j.polymdegradstab.2007.06.017

other additives are incorporated into a molten thermoplastic to produce a homogeneous composite material. Composite material is then formed into a product. Common forming methods include profile extrusion (extruding molten composite through a die), injection molding (injecting molten composite into a three-dimensional mold), and compression molding (pressing molten composite between two mold halves). Inline manufacturing occurs when compounding and forming are done in a single process [2]. The manufacturing method used directly influences composite surface characteristics [3,4].

The growth in exterior applications results in a need to understand the durability of WPCs. Durability issues such as weatherability, moisture resistance, thermal performance, fungal attack, and fire performance need to be addressed. Of specific interest is weatherability, and several research groups have been working on characterizing and understanding changes that occur when WPCs weather [4–14].

It has been shown that the color of WPCs lightens during weathering [4–9]. Amount or rate of lightening can change depending upon manufacturing method, exposure type, and photostabilization system added. Manufacturing method directly influences surface characteristics of WPCs, and their response to weathering. In a previous study we demonstrated that WPCs with similar formulations manufactured differently, using injection molding or extrusion, influenced the rate of change in lightening (i.e., rate of increase in L^* value in the CIE $L^*a^*b^*$ color space) [4]. Injection molded composites lightened more slowly upon weathering than extruded composites, largely due to a hydrophobic character of the HDPE-rich layer that formed on the surface of composite during injection molding. This delayed some changes that occurred to the composite during weathering.

The presence of moisture greatly contributes to WPC lightening during weathering. When WPCs were exposed to xenon-arc radiation either with or without water spray in an accelerated weathering apparatus, lightening has been shown to be more evident when composites were exposed to both xenon-arc radiation and water spray as opposed to xenon-arc radiation only [5]. Ultraviolet radiation can lighten WPCs by causing the surface of the polymer matrix to crack, creating a whitening effect, and to a larger extent, by bleaching wood particles. Although ultraviolet radiation contributes to wood particle bleaching, the presence of water exacerbates the problem. Water accelerates oxidation reactions and causes the wood fiber to swell creating more openings for light penetration. Additionally, water can remove some water soluble extractives that impart color to the wood particle. Photostabilizers are commonly added to stabilize the color of WPCs. Ultraviolet absorbers, light stabilizers, and pigments can alter color changing characteristics of WPCs [6–9].

The surface chemistry of WPCs also changes during weathering. Fourier transform infrared (FTIR) spectroscopy is one tool that can be used to determine changes in chemistry at the composite surface during weathering. Peaks that appear on the spectra can be assigned to functional groups present at the composite surface. Oxidation at the surface is one measure of surface degradation, and can be followed throughout weathering [7,9–13]. While spectroscopic methods are useful for determining WPC surface oxidation, they cannot distinguish between surface oxidation of the HDPE or of the wood particle.

In this study, wood flour/polyethylene composites were manufactured via injection molding and extrusion. The objective of this study was to gain insight into how the surface of WPCs changes during weathering. To accomplish this, we determined surface characteristics of WPCs before and after weathering. This was accomplished visually by examining scanning electron micrographs combined with surface analysis techniques including Fourier transform infrared (FTIR) spectroscopy, X-ray photoelectron spectroscopy (XPS) and contact angle measurements.

2. Experimental methods

2.1. Materials

The materials used in this study were wood flour (WF) and high-density polyethylene (HDPE). The WF supplied was 40-mesh pine (AWF 4020, American Wood Fibers, Schofield, WI). The HDPE was purchased as virgin material with a melt index of 0.72 g/10 min and density of 0.963 g/cm^3 (Fortiflex A60-70-162, Solvay Polymers, Inc., Houston, TX). To aid in processing extruded composites, a lubricant, consisting of a blend of fatty acid metal soap and an amide, was also used (TR016, density = 0.98 g/cm^3, Struktol, Stow, OH). The WPCs were not stabilized to better determine changes in surface due solely to manufacturing method and weathering.

2.2. Processing

2.2.1. Injection molded

WF was dried for 24 h at 105 °C; HDPE and WF were then dry-blended at 50% WF based on total composite weight. Compounding was accomplished using a 32-mm Davis Standard (Pawcatuck, CT) twin-screw extruder to produce homogeneous WF/HDPE composite pellets. Melt temperature at the die was 200 °C and melt pressure was 2.96 MPa. Pellets were dried at 105 °C for at least 24 h prior to injection molding into flexural bar test samples. Composites were injection molded using a 33-ton Cincinnati Milacron (Batavia, OH) injection molder. The mold nozzle temperature was 204 °C, and injection pressure reached a peak of 12.4 MPa. The American Society for Testing and Materials (ASTM) mold cavity used for flexural samples was 120 × 3 × 12 mm [15].

2.2.2. Extruded and planed

Extruded composites were manufactured using a Davis Standard 94-mm Woodtruder in conjunction with a die that produced a 30- by 140-mm radius edge profile. This was a direct extrusion method where wood flour was dried using a twin-screw extruder. HDPE and additives were melted using a single screw extruder. Dried WF from the twin-screw extruder was combined with molten HDPE in a single step.

Remaining moisture was removed by vacuum venting. The composite was 49% by weight WF, 8% by weight lubricant, and the remainder HDPE. The die temperature was 180 °C, and die pressure was 2.1 MPa. Flexural test specimens (120 × 3 × 12 mm) intended to evaluate the extruded surface were cut from deck boards for testing, leaving the extruded surface intact (Fig. 1).

The planed test specimens were also cut from the larger extruded composites as shown in Fig. 1. Less than 1 mm of the surface of extruded composites was planed to remove any surface characteristics resulting from the extrusion processing method. Samples were cut from the deck board just below the planed surface (Fig. 1) to evaluate possible differences in weathering between extruded surfaces and material beneath the extruded surface.

2.3. Testing and analysis

2.3.1. Weathering

Composites were placed in a xenon-arc type light exposure apparatus operated according to ASTM D 2565 [16]. Samples were mounted in four rows on a drum that rotated around a xenon-arc bulb filtered with Type S borosilicate filters at 1 rpm. Each 2-h weathering cycle consisted of 108 min of UV exposure and 12 min of simultaneous water spray and UV exposure [16]. An irradiance sensor was used to measure light intensity for wavelengths from 300 to 400 nm. Irradiance (W/m^2) was monitored and voltage to the bulb was changed periodically to maintain constant irradiance. Radiant energy, or amount of light energy to which samples were subjected was calculated (irradiance × time). Samples were removed for analysis after 3000 h of weathering. At that time the total radiant energy to which the specimens were exposed was 439 MJ/m^2 at 300–400 nm.

2.3.2. Scanning electron microscopy

Composite surfaces were sputtered with gold and analyzed with a scanning electron microscope (SEM) (JSM-840, JEOL USA, Inc., Peabody, MA) at a working distance of approximately 25 mm, voltage of 15 kV, and probe current of 1×10^{-9} A.

2.3.3. Density

Samples were dried for 24 h at 105 °C before being tested for density according to ASTM D 792 [17]. The sample size was approximately 60 × 3 × 12 mm. Twenty replicates of each composite before and after weathering were tested.

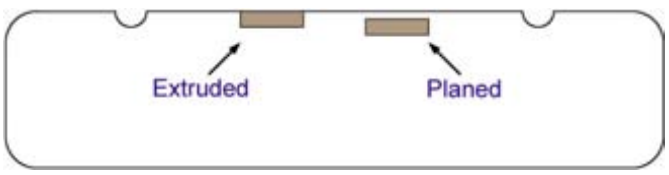

Fig. 1. Extruded profile showing cutting sites for extruded and planed composite samples.

2.3.4. Fourier transform infrared spectroscopy

FTIR spectroscopy was conducted on a Mattson Genesis II (Thermo Electron Corp., Madison, Wisconsin) spectrometer to provide knowledge of functional groups present at the composite surface before and after weathering. For each sample, 100 scans were recorded in absorbance units from 4000 to 700 cm^{-1}. Spectra were obtained using attenuated total reflectance (ATR). Composite surfaces analyzed were in contact with a ZnSe crystal with a 45° angle of incidence. At least five replicate samples were analyzed.

Wood spectra have a strong peak at 1023 cm^{-1} as a result of C–O stretching in cellulose and C–O deformation in lignin [18–20]. A wood index, defined in a previous study was calculated using Eq. (1) [4]:

$$\text{Wood index} = \frac{I_{1023}}{I_{2912}} \times 100 \quad (1)$$

where I represents peak intensity. Peak intensity was normalized using the peak at 2912 cm^{-1}, which corresponds to alkane CH stretching vibrations of methylene groups ($-CH_2-$).

2.3.5. Contact angle

A Ramé-Hart Goniometer (Netcong, NJ) was used to determine contact angle of the composites' surface. A drop of distilled water was placed on the composite surface, and contact angle was determined using the Ramé-Hart Imaging 2001 software package. Contact angle was measured every second, the average of the first 10 measurements is reported. Contact angle was measured for at least five specimens of each composite, and two locations per specimen.

2.3.6. X-ray photoelectron spectroscopy (XPS)

X-ray photoelectron spectra were collected using a Perkin Elmer Phi 5400 ESCA system (Waltham, MA) with a Magnesium Kα X-ray source. Samples were analyzed at pressures between 10^{-9} and 10^{-8} Torr with a pass energy of 29.35 eV and a take-off angle of 45°. The spot size was roughly 250 μm^2. Three types of spectrum were collected: a survey spectrum, a low-resolution spectrum from 0 to 1100 eV binding energy, and a high-resolution spectrum of the C_{1s} region from 280 to 300 eV. To determine types of oxygen–carbon bonds present, chemical bond analysis of carbon was accomplished by curve fitting the C_{1s} peak and deconvoluting it into four subpeaks. Deconvoluted peak assignments with corresponding binding energy and bond type are shown in Table 1. An oxygenated to unoxygenated carbon ratio ($C_{ox/unox}$) was calculated using Eq. (2) [10].

Table 1
Deconvoluted peak assignments with corresponding theoretical binding energy and bond type for high-resolution XPS scan of C_{1s}

Carbon group	Binding energy (eV)	Bond
C1	285.0	C–C or C–H
C2	286.5	C–O
C3	288.0	O–C–O or C=O
C4	289.5	O–C=O

$$C_{ox/unox} = \frac{C_{oxygenated}}{C_{unoxygenated}} = \frac{C2 + C3 + C4}{C1} \quad (2)$$

2.3.7. Statistics

Each bar shown in Figs. 3, 6, and 7 represents the mean of that data set and error bars represent one standard deviation. To determine significant differences between compared means, Student's two-tailed *t*-tests, assuming unequal variance, were carried out at $\alpha = 0.05$. Letters above each bar in these figures denote significance. If the letters are the same, the hypothesis that the means were the same was accepted. In other words the two means are not significantly different. The converse is that if the letters are different, the means are significantly different.

3. Results and discussion

Micrographs of the surfaces of injection molded, extruded, and planed composite surfaces before and after weathering are shown in Fig. 2. Before exposure the injection molded composite surface (Fig. 2a) was relatively smooth, and HDPE flow over wood particles was evident. The extruded composite surface (Fig. 2c) had more voids where HDPE failed to encapsulate wood particles than injection molded surfaces. During extrusion the lower processing pressure and temperature did not permit HDPE to flow as well at the surface as did higher processing pressure and temperature used for injection molded composites. Planed surfaces of the extruded composites (Fig. 2e) had a smoother surface than the original extruded surface. However, wood particles exposed at the surface during planing are evident.

After weathering for 3000 h the surface of each composite was degraded (Fig. 2b, d and f). Cracks appeared in the HDPE matrix. In addition, wood particles protruded from the composite surface. Extruded and planed composite surfaces were more degraded by weathering than the injection molded composite surface. Photodegradation of HDPE can cause surface cracking [11]. However, the protrusion of wood particles was likely a result of the wood particles swelling and shrinking after absorbing and desorbing moisture. This action could result in voids at the wood flour/HDPE interface and cracks in the HDPE matrix. In this study, surface cracking was likely due to both HDPE photodegradation and wood particle swelling because the composites were unstabilized. Stabilization of HDPE can successfully inhibit surface cracking during weathering; however, some surface cracking of WPCs occurs during weathering even when the HDPE is stabilized [11]. Therefore, surface degradation of WPCs is a complex combination of degradation of HDPE due to exposure to xenon-arc radiation and of changes in wood particles due to the combination of exposure to xenon-arc radiation and water spray.

The density of the composites before and after weathering is shown in Fig. 3. Initially, injection molded composites had a slightly higher density than extruded and planed composites. This is likely due to higher processing pressure used during injection molding. After exposure, density of each of the composites decreased. This is consistent with the surface characteristics shown using SEM. It is likely that as the surface cracked and flaked off, voids appeared at the surface and the wood/HDPE interface and the overall density of each type of composite decreased.

Each composite surface was examined using FTIR spectroscopy. The peaks of most interest to us were 3318 cm^{-1}, 2912 cm^{-1}, and 1023 cm^{-1}. FTIR has been used to characterize the surface of wood [18–20]. The broad peak that occurs at 3400–3200 cm^{-1} is associated with –OH stretching in hydroxyl groups originating mainly from cellulose [18,19]. The peak at 2912 cm^{-1} is assigned to CH stretching in $-CH_2-$ groups [18,19]. The peak at 1023 cm^{-1} is associated with both the C–O stretch in cellulose and the C–O deformation in the primary alcohols of lignin [18,19]. We previously examined FTIR spectra for southern yellow pine (SYP, *Pinus* spp) and HDPE [4]. The peak at 2912 cm^{-1} appeared as a very strong peak in HDPE and a much weaker peak in SYP. Compared to SYP, a relatively large proportion of HDPE consisted of $-CH_2-$ groups. The peak at 1023 cm^{-1} was dominant in the SYP spectra, but not present in the spectra of HDPE. These two peaks were used to define a wood index as a ratio of peak height at 1023 cm^{-1} to peak height at 2912 cm^{-1}, multiplied by 100 (Eq. (1)) [4].

Figs. 4 and 5 show FTIR spectra obtained for injection molded, extruded, and planed composites before and after weathering, respectively. Peaks at 3318 cm^{-1} and 1023 cm^{-1} were larger for planed composites compared with extruded and injection molded composites. Clearly the surface of the planed composites exhibits more of a wood characteristic than the extruded and injection molded composites, respectively. By comparison, this suggests the presence of an HDPE-rich layer on the injection molded composite surface. SEM micrographs suggested that wood present at the surface of injection molded composites was minor compared to HDPE present (Fig. 2a), and wood particles at the surface of planed composites were readily apparent (Fig. 2e). After weathering, FTIR peaks at 3318 cm^{-1} and 1023 cm^{-1} were greatly diminished for each of the composites (Fig. 5), indicating a loss of wood at the composite surface.

Wood index (Eq. (1)) as a function of manufacturing method and exposure is shown in Fig. 6. Before exposure, planed composites had the highest wood index, followed by extruded and injection molded composites. This is consistent with trends observed with SEM and FTIR, higher injection pressures resulted in less wood at the injection molded composite surface compared with extruded composites, and surface wood particles were exposed during planing. After weathering, the wood index for each of the composites decreased. As weathering occurs swelling wood particles constrained by the HDPE matrix results in swelling pressures that simultaneously cause microcracks in the matrix at the interface and fracture wood particles. Fractured and loose wood particles are washed away during the accelerated weathering water spray cycle. The decrease in the wood index confirms a loss of wood at the composite surface.

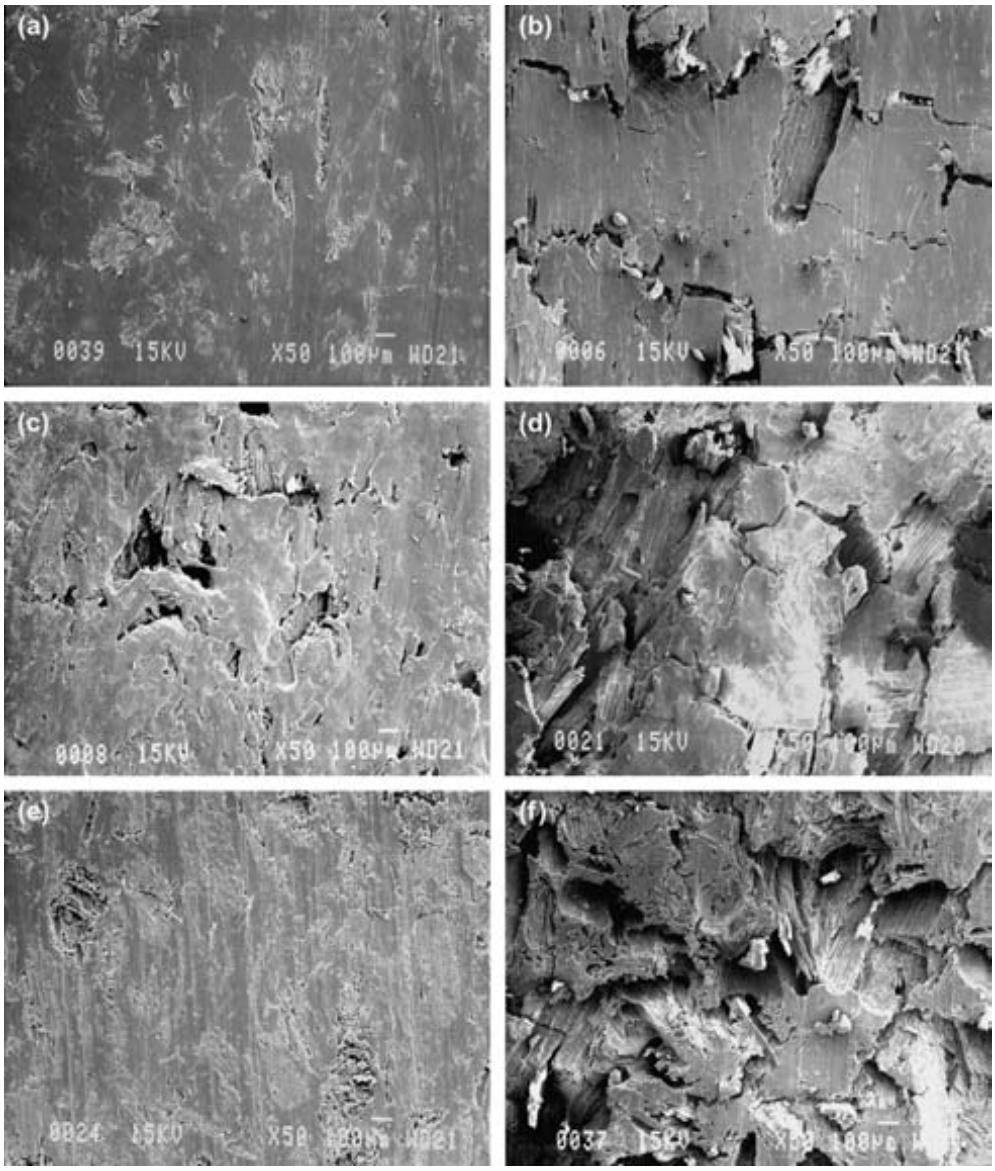

Fig. 2. Scanning electron micrographs of injection molded, extruded, and planed WF/HDPE composite surfaces before weathering (a,c,e), and after 3000 h of accelerated weathering (b,d,f).

Contact angle was measured after placement of a drop of liquid on the composite surface to determine relative wettability. Wood, a hydrophilic material, has a lower contact angle than HDPE, a hydrophobic material. Because planed composites have a high wood index, i.e., more wood at the surface, we expected that planed composites would also have the lowest contact angle compared with extruded and injection molded composites. However, our experimental results indicated that both planed and extruded composites had a high contact angle compared with injection molded composites (Fig. 7). This was likely due to composite formulation. During extrusion, a lubricant was added to the composite to aid in profiling. The lubricant was a proprietary blend of fatty acid metal soap and an amide. Because contact angles of both extruded and planed composites were not significantly different, lubricant is likely distributed throughout the composite surface layer.

Based on the results of FTIR analysis, we expected contact angle to increase after weathering. As the hydrophilic wood component of the WPCs was washed away during weathering, the surface became HDPE-rich, i.e, more hydrophobic, as shown in wood index (Fig. 6). After weathering, contact angle of injection molded and planed composites increased but did not change for extruded composites (Fig. 7). Loss of wood particles from the injection molded composite surface likely corresponds with an increase in contact angle. However, extruded and planed composites experienced an additional change that influenced contact angle. Surface erosion during weathering likely resulted in a loss of lubricant, resulting in a decrease in contact angle, in addition to a loss of wood particles, resulting in an increase in contact angle. For extruded composites, these losses may have cancelled each other out, resulting in no significant change in contact angle. Planed

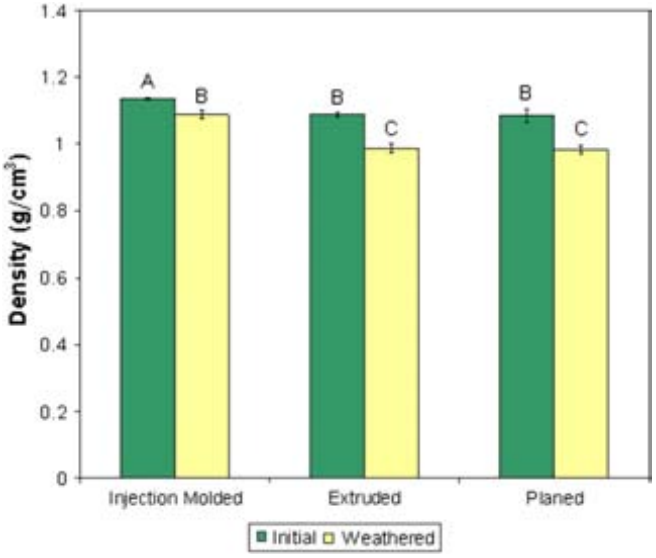

Fig. 3. Density of injection molded, extruded, and planed WF/HDPE composites before and after accelerated weathering. Letters above bars denote significance, i.e., a common letter indicates that the difference between the two means is not statistically significant.

composites, with more wood at the surface initially and less lubricant, experienced more surface erosion, thus contact angle increased as degraded wood component was removed.

XPS was employed to confirm that lubricant was present at the surface of extruded and planed composites. A low-resolution scan yielded elemental composition of the composite surface (Table 2). Unexposed extruded and planed

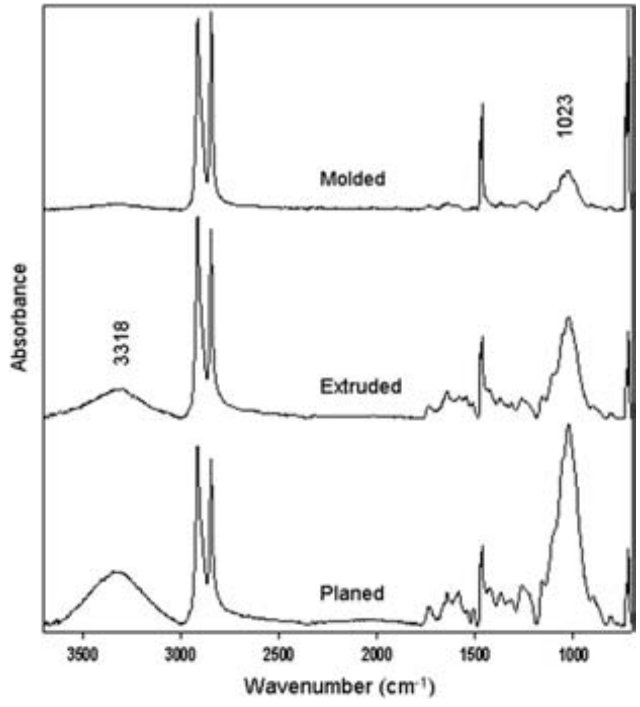

Fig. 4. FTIR spectra of injection molded, extruded, and planed WF/HDPE composite surfaces before weathering. Peaks at 3318 and 1023 cm^{-1} are assigned to the wood component.

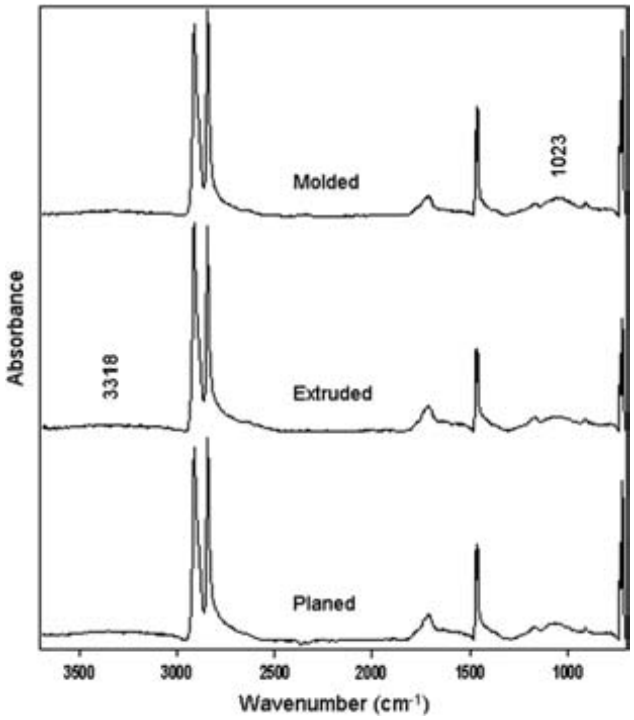

Fig. 5. FTIR spectra of injection molded, extruded, and planed WF/HDPE composite surfaces after 3000 h of accelerated weathering. Peaks at 3318 and 1023 cm^{-1} are assigned to the wood component.

composite surfaces had calcium present and a higher carbon content than unexposed injection molded composite surfaces. This is consistent with the presence of lubricant, a fatty acid metal soap. A fatty acid consists of an aliphatic chain (i.e., high in $-CH_2-$) with a carboxylic acid end. In a metal soap, the hydrogen of the carboxylic acid is replaced, often with calcium. Both the presence of calcium, and increase in carbon, suggest that lubricant is present at the surface of

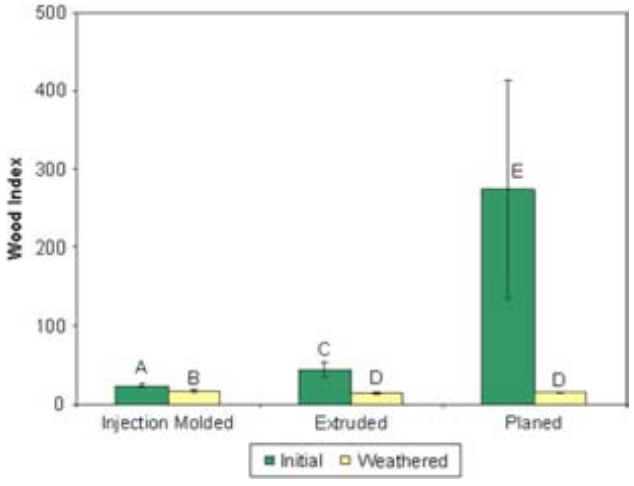

Fig. 6. Calculated wood index for injection molded, extruded, and planed WF/HDPE composites before and after accelerated weathering. Letters above bars denote significance, i.e., a common letter indicates that the difference between the two means is not statistically significant.

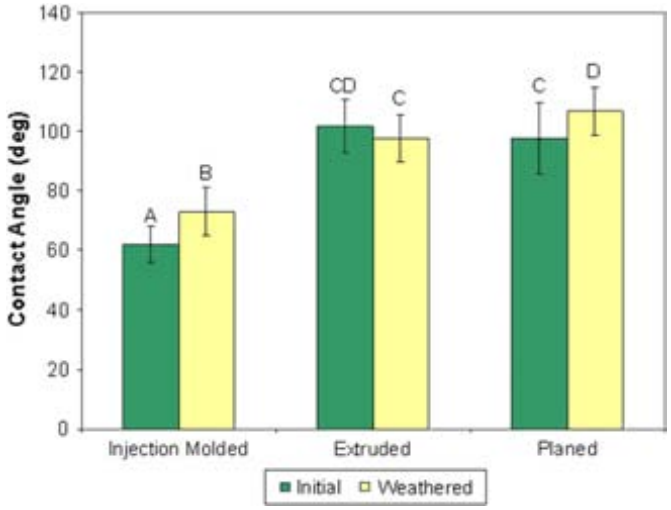

Fig. 7. Contact angle of injection molded, extruded, and planed WF/HDPE composites before and after accelerated weathering. Letters above bars denote significance, i.e., a common letter indicates that the difference between the two means is not statistically significant.

both extruded and planed composites. The aliphatic chain is hydrophobic, which also supports the increase in contact angle compared with injection molded composites. After weathering, calcium was no longer present at the extruded or planed composite surface. The disappearance of calcium suggests that lubricant was removed during surface erosion, or the metal soap was converted to free acid. The change in contact angle further supports that lubricant was no longer influencing composite surface characteristics.

Deconvolution of the carbon peak showed that relative amount of C1 carbon group, representing a C–C or C–H bond decreased after weathering for each of the composites (Table 3). However, concentration of unoxidized carbon atoms ($C1$) remained higher for both extruded and planed samples compared to injection molded ones, accounting for the greater contact angle values observed for extruded and planed samples. XPS data listed in Table 3 also shows an increase in total oxygenated carbon bonds, $C_{ox/unox}$, suggesting that surface oxidation occurred. Since FTIR results showed a decrease in peaks associated with wood components (Figs. 4 and 5), this increase in total oxygenated carbon bonds may be attributed to degradation of the matrix.

It should be mentioned that although both FTIR and XPS are techniques used to determine surface chemistry, penetration depth of XPS is less than FTIR. As such, XPS is a more surface sensitive technique than FTIR. Each technique has strengths and weaknesses. For example, the composite surface may be oxidizing as shown by XPS, while the surface layer is experiencing a decrease in oxygenated functional groups, as shown by FTIR. XPS also was sensitive to the presence of lubricant at the composite surface, which was consistent with the contact angle results. FTIR was able to characterize the morphology of the composite surface as well as the loss of wood particles from the surface, which was consistent with the SEM results.

Table 2
Elemental composition at composite surface determined by low-resolution XPS scan

Sample	Elemental composition (%)				
	C_{1s}	N_{1s}	O_{1s}	Si_{2p}	Ca_{2p}
Injection molded (initial)	81.6	1.5	15.3	1.7	–
Injection molded (weathered)	84.8	1.8	12.9	0.5	–
Extruded (initial)	84.0	1.5	10.9	2.8	0.9
Extruded (weathered)	86.6	–	13.4	–	–
Planed (initial)	87.0	1.8	9.7	1.0	0.5
Planed (weathered)	87.3	1.0	11.7	–	–

Table 3
Relative amount of different carbon-to-oxygen bonds at composite surface determined by high-resolution XPS

Sample	Analysis of C_{1s} peaks (%)				
	$C1$	$C2$	$C3$	$C4$	$C_{ox/unox}$
Injection molded (initial)	83.8	11.5	2.7	2.1	0.19
Injection molded (weathered)	80.9	12.5	3.9	2.7	0.24
Extruded (initial)	86.6	9.5	3.0	0.9	0.16
Extruded (weathered)	84.5	11.5	2.6	1.4	0.18
Planed (initial)	86.7	9.6	1.6	2.0	0.15
Planed (weathered)	83.3	9.8	3.9	3.1	0.19

4. Conclusions

As wood flour filled HDPE composites weather, they undergo changes in surface characteristics. Exposure to water causes wood particles to swell. This creates microcracks in the matrix, degrades the wood/HDPE interface, and shears the wood particle, resulting in composite density reduction. Photodegradation also causes surface cracking of the matrix and degradation of the lignin portion of the wood particle. As a result, loose wood particles, loose cellulose at the wood surface, and degraded lignin are washed away.

Composite surface erosion was shown using SEM. Wood flour filled HDPE composites manufactured by different processes have different surface characteristics. SEM micrographs clearly showed that injection molded composites have more of a polymer rich surface layer compared with extruded composites. They have shown that the surface of extruded and planed composites degraded more than the surface of injection molded composites after 3000 h of weathering in an accelerated weathering apparatus.

Fourier transform infrared (FTIR) spectroscopy was used to identify functional groups present at the surface of WPCs. By following peaks assigned to wood components, it was possible to identify differences in composite surface characteristics based on manufacturing method, and follow the loss of wood from the composite surface after weathering. Wood index was useful to determine relative amounts of wood at the composite surface and to characterize loss in wood from the surface. However, wood index did not relate directly to contact angle values. Lubricant, a component confirmed present at the surface of extruded and planed composites using XPS, influenced contact angle such that contact angle of extruded and

planed composites was larger than for injection molded composites. Although the defined wood index can be a good indicator of how the surface of WPCs will erode, small amounts of additives may influence surface wettability. Therefore, these surface analysis techniques must be used together to develop a full understanding of changes that occur at the composite surface after weathering.

Acknowledgement

The authors gratefully acknowledge American Wood Fibers and Struktol for their donation of materials.

References

[1] Rossi L. WPCs: putting innovation on a faster track. In: Proceedings, eighth international conference on woodfiber–plastic composites. Madison, WI; 23–25 May 2005.
[2] Clemons CM. Wood–plastic composites in the United States: the interfacing of two industries. Forest Prod J 2002;52(6):10–8.
[3] Clemons CM, Ibach RE. Effects of processing method and moisture history on laboratory fungal resistance of wood–HDPE composites. Forest Prod J 2004;54(4):50–7.
[4] Stark NM, Matuana LM, Clemons CM. Effect of processing method on surface and weathering characteristics of wood-flour/HDPE composites. J Appl Polym Sci 2004;93(3):1021–30.
[5] Stark NM. Effect of weathering cycle and manufacturing method on performance of wood flour and high-density polyethylene composites. J Appl Polym Sci 2006;100(4):3131–40.
[6] Falk RH, Lundin T, Felton C. The effects of weathering on wood–thermolastic composites intended for outdoor application, Proceedings, durability and disaster mitigation in wood–frame housing. Madison, WI: Forest Products Society; 6–8 Nov 2000. p. 175–179.
[7] Matuana LM, Kamdem DP, Zhang J. Photoaging and stabilization of rigid PVC/wood–fiber composites. J Appl Polym Sci 2001;80(11):1943–50.
[8] Stark NM, Matuana LM. Ultraviolet weathering of photostabilized wood-flour-filled high-density polyethylene composites. J Appl Polym Sci 2003;90(10):2609–17.
[9] Muasher M, Sain M. The efficacy of photostabilizers on the color change of wood filled plastic composites. Polym Degrad Stab 2006;91(5):1156–65.
[10] Stark NM, Matuana LM. Surface chemistry changes of weathered HDPE/wood-flour composites studied by XPS and FTIR spectroscopy. Polym Degrad Stab 2004;86(1):1–9.
[11] Stark NM, Matuana LM. Surface chemistry and mechanical property changes of wood-flour/high-density-polyethylene composites after accelerated weathering. J Appl Polym Sci 2004;94(6):2263–73.
[12] Seldén R, Nystrom B, Långström R. UV aging of poly(propylene)/wood-fiber composites. Polym Compos 2004;25(5):543–53.
[13] Colom X, Cañavate J, Pagès P, Saurina J, Carrasco F. Changes in crystallinity of the HDPE matrix in composites with cellulosic fiber using DSC and FTIR. J Reinf Plast Compos 2000;19(10):818–30.
[14] Matuana LM, Kamdem DP. Accelerated ultraviolet weathering of PVC/wood-flour composites. Polym Eng Sci 2002;42(8):1657–66.
[15] ASTM D 790, Annual book of ASTM standards. 8.01. Conshohocken, PA: American Soc. Testing Mat.; 2004.
[16] ASTM D 2565, Annual book of ASTM standards. 8.02. Conshohocken, PA: American Soc. Testing Mat.; 2004.
[17] ASTM D 792, Annual book of ASTM standards. 8.02. Conshohocken, PA: American Soc. Testing Mat.; 2004.
[18] Baeza J, Freer J. In: Hon DN-S, Shiraishi N, editors. Chemical characterization of wood and its components: wood and cellulosic chemistry. New York: Marcel Dekker; 2001. p. 275–382 [chapter 8].
[19] Pandey KK. A study of chemical structure of soft and hardwood and wood polymers by FTIR spectroscopy. J Appl Polym Sci 1999;71(12):1969–75.
[20] Tshabalala MA. Surface characterization. In: Rowell RM, editor. Handbook of wood chemistry and wood composites. Boca Raton: CRC Press; 2005. p. 187–211 [chapter 8].